Climatology of the Residual Mean Circulation of the Martian Atmosphere and Contributions of Resolved and Unresolved Waves Based on Reanalysis Data

Anzu. Asumi, **Kaoru. Sato**, and **Masashi. Kohma**, *Department of Earth and Planetary Science, Graduate School of Science, The University of Tokyo, Tokyo, Japan (asumi@eps.s.u-tokyo.ac.jp)*, **Yoshi-Yuki. Hayashi,** *Department of Planetology/Center for Planetary Science, Graduate School of Science, Kobe University, Hyogo, Japan*.

1. Introduction

Lagrangian mean circulation of planetary atmosphere is important in determining not only the distribution of mass and minor constituents but also the temperature structure that are warmer or cooler than those expected from the radiative equilibrium. For the Martian atmosphere, the Lagrangian mean circulation has been studied using several spacecraft temperature observations and Mars general circulation models (MGCM) so far. However, in most of these studies, the analysis was made only for a specific season or event such as a global dust storm (GDS). In this study, the climatology of the Lagrangian mean circulation and its driving mechanism is examined using recently available long-term reanalysis dataset, EMARS [1] based on the transformed Eulerian mean (TEM) equations theory [2]. This theory describes the interaction between waves and mean flow and hence is useful for the analysis regarding the momentum budget of the atmospheric circulation.

According to the TEM equations theory, the wave forcing due to large-scale waves that are explicitly expressed in the reanalysis, hereafter referred to as resolved wave (RW), can be estimated directly as the divergence of the Eliassen–Palm (EP) flux. Kuroda et al. (2016)[2] used a high resolution GCM and suggested that the contribution of gravity waves (GWs) resolved in the model increases in simulations with higher model resolution. Thus, we quantitatively examine the wave forcing associated not only with RWs in EMARS but also with unresolved waves (UWs) including subgrid-scale GWs, which contribute to the residual mean circulation as a good approximation of the Lagrangian mean circulation. UW contribution is indirectly estimated by applying the method devised originally for a study of Earth's middle atmosphere, as described in Sato and Hirano (2019)[3].

Additionally, during a GDS event, significant warming is observed in the winter polar region. A possible mechanism is adiabatic heating associated with intensified downwelling. Therefore, we investigate the changes in the Lagrangian mean circulation owing to the GDS event, as a case study for the GDS in MY28.

2. Method of estimating UWs:

We will provide a brief explanation of the indirect method of UW contribution to the residual mean flow. See Asumi et al. (2025)[4] for the details. The zonal mean momentum equation is expressed as

$$\frac{\partial \bar{u}}{\partial t} - \hat{f}\bar{v}^* + \bar{w}^* \frac{\partial \bar{u}}{\partial z} = \frac{1}{\rho_0 a \cos\phi} \nabla \cdot \boldsymbol{F} + \bar{\mathrm{X}}. \quad (1)$$

Wave forcing due to RWs ($\nabla \cdot \boldsymbol{F}_{(\mathrm{RW})}$) is a part of $\nabla \cdot \boldsymbol{F}$.

$$\nabla \cdot \boldsymbol{F} = \nabla \cdot \boldsymbol{F}_{(\mathrm{RW})} + \nabla \cdot \boldsymbol{F}_{(\mathrm{UW})} \quad (2)$$

The term $\nabla \cdot \boldsymbol{F}_{(\mathrm{UW})}$ is the sum of the parameterized GW forcing, the assimilation increment which is composed of the GW forcing that is not properly expressed by the GW parameterization, and other model deficiency. By integrating each term in Eq (1) along the contours of absolute angular momentum,

$$\bar{m} = a\cos\phi\,(\bar{u} + a\cos\phi\,\Omega), \quad (3)$$

the contribution of UWs ($\bar{\Psi}^*_{\nabla\cdot\boldsymbol{F}_{(\mathrm{UW})}}(\phi, z)$) to $\bar{\Psi}^*(\phi, z)$ is indirectly estimated as follows:

$$\bar{\Psi}^*(\phi, z) = -\cos\phi \int_z^\infty \rho_0 \bar{v}^* dz \quad (4)$$

$$\bar{\Psi}^*_{\nabla\cdot\boldsymbol{F}_{(\mathrm{RW})}}(\phi, z) = -\int_z^\infty \left[\frac{\nabla\cdot\boldsymbol{F}_{(\mathrm{RW})}}{a\hat{f}}\right]_{\bar{m}} d\zeta \quad (5)$$

$$\bar{\Psi}^*_{\bar{u}_t}(\phi, z) = \cos\phi \int_z^\infty \left[\frac{\rho_0}{\hat{f}}\frac{\partial \bar{u}}{\partial t}\right]_{\bar{m}} d\zeta \quad (6)$$

$$\bar{\Psi}^*_{\nabla\cdot\boldsymbol{F}_{(\mathrm{UW})}}(\phi, z) = \bar{\Psi}^*(\phi, z) - \bar{\Psi}^*_{\nabla\cdot\boldsymbol{F}_{(\mathrm{RW})}}(\phi, z) - \bar{\Psi}^*_{\bar{u}_t}(\phi, z) \quad (7)$$

3. Results

Figure 1a shows the climatology of the residual mean meridional flow $\bar{v}^*$ overlaid with the absolute angular momentum $\bar{m}$ for the northern hemisphere (NH) winter. A strong northward $\bar{v}^*$ is observed with a peak of 28.5 m s^{-1} at 20°N, z = ~60 km (Figure 1a). Such strong $\bar{v}^*$ are not attributed to the Hadley circulation because the area, where the $\bar{m}$ contours and $\bar{\Psi}^*$ are parallel, is limited below ~45 km (not shown). In the latitudes of ~0°–30°N and altitudes between ~45–80 km, the latitudinal gradient of $\bar{m}$ is quite small. In this region, $\bar{v}^*$ can take any value. The reason why the $\bar{v}^*$ maximum is located at ~60km is that the wave forcings in the latitudes of ~30°S – 0° and the latitudes of 35°–70°N are strongest near 60 km in the vertical.

Figure 1b shows the climatology of the resolved wave forcing $\nabla \cdot \boldsymbol{F}_{(\mathrm{RW})}$ overlaid with the residual mean meridional flow. In mid- and high latitudes of both NH and SH, the sign of the $\nabla \cdot \boldsymbol{F}_{(\mathrm{RW})}$ between 20 and 80 km (Figure 1b) is roughly consistent with that of $\bar{v}^*$: poleward flow in NH high latitudes is driven by the negative $\nabla \cdot \boldsymbol{F}_{(\mathrm{RW})}$, while equatorward flow in SH mid latitudes is driven by the positive $\nabla \cdot \boldsymbol{F}_{(\mathrm{RW})}$.

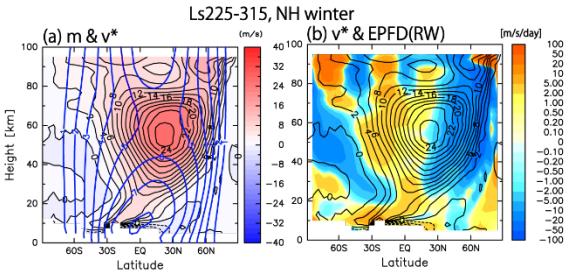

Figure 1. Latitude-height section of (**a**) the residual mean flow $\bar{v}^*$ (color) and the absolute angular momentum (blue counters) $\bar{m}$ and (**b**) the EP-flux divergence $\nabla \cdot \boldsymbol{F}_{(RW)}$ (color) and $\bar{v}^*$ (counters)

Figure 2 shows the climatology of $\bar{\Psi}^*$, $\bar{\Psi}^*_{\nabla\cdot\boldsymbol{F}_{(\mathrm{RW})}}$, and $\bar{\Psi}^*_{\nabla\cdot\boldsymbol{F}_{(\mathrm{UW})}}$ for the NH winter in the latitude-height section. The overall structure of $\bar{\Psi}^*$ is mainly determined by that of $\bar{\Psi}^*_{\nabla\cdot\boldsymbol{F}_{(\mathrm{UW})}}$. In the NH, the contribution of RWs to the large clockwise circulation is only about 20 % that of UWs. In the SH, the anti-counter-clockwise circulation below 50km over the mid- and high latitudes is explained mainly by the RW contribution, although the clockwise circulation above 50km is determined by $\bar{\Psi}^*_{\nabla\cdot\boldsymbol{F}_{(\mathrm{UW})}}$. A small clockwise circulation at 60°S–80°S below 30 km is also attributable to $\bar{\Psi}^*_{\nabla\cdot\boldsymbol{F}_{(\mathrm{UW})}}$. It should be noted that the strength of $\bar{\Psi}^*_{\bar{u}_t}$ is weak, and thus it is also not shown here.

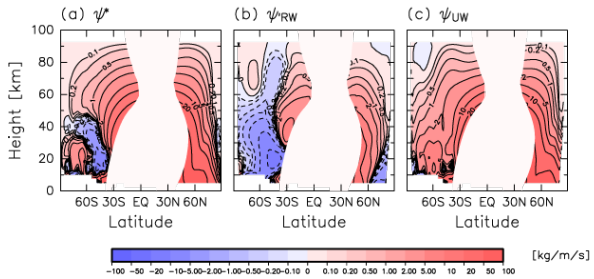

Figure 2. Latitude-height sections of the NH winter climatology of (a) the residual mean stream function, and the contribution of (b) RWs and (c) UWs.

Figure 3 provides comparisons between the GDS period (MY28) and the climatology (MY29–32) in the meridional cross section regarding the zonal mean temperature (Figures 3a–3c) and residual mean mass stream function overlaid with the blue counters of absolute angular momentum per unit mass (Figures 3d–3f). The characteristics in the GDS period are considerably different from the climatology. The high temperature anomaly in all latitudes of SH and low and mid-latitudes of NH is likely caused mainly by diabatic heating due to solar radiation absorption by a significant amount of airborne dust. During the GDS, dust is transported upward by the enhanced global circulation and reaches a quite high altitude of ~60 km all over the planet. However, the significantly high temperature anomaly observed in NH high latitudes is not due to diabatic heating because of little solar radiation but probably results from adiabatic heating associated with the strongly enhanced downwelling as suggested by many previous studies and expected from the stream function anomaly (Figure 3f). Different mechanisms of the strong enhancement of the downwelling during the GDS period are considered for two altitude regions below and above 60 km. Below z = 60 km, the $\bar{m}$ conserving Hadley-like cell exists with its latitudinal extent reaching near the north pole (Figure 3d), resulting in strengthening the downward branch. Above z = ~60 km, the considerably strong $\bar{v}^*$ reaches near the north pole (not shown here). The flow is not attributed to Hadley-like circulation because it crosses the $\bar{m}$ contours. Instead, the downwelling above 60km is attributed to the considerably stronger wave-driven meridional flow extending to the north pole. Estimation of the wave forcing due to UWs in the reanalysis data, including subgrid-scale gravity waves, reveals that the strong meridional flow is driven by the UWs rather than RWs.

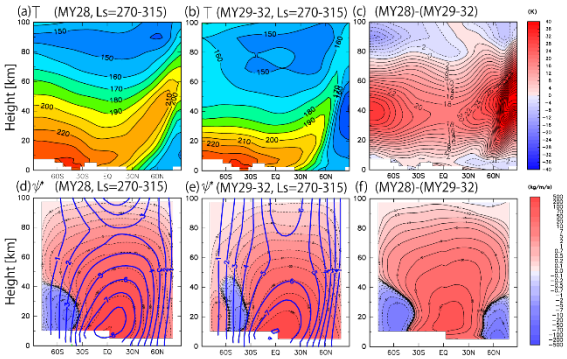

Figure 3. Latitude-height section of zonal mean temperature for (a) the GDS period ($Ls = 270° - 315°$ in MY28), (b) the climatology, and (c) the difference between (a) and (b). (d)–(f): Same as (a)–(c) but for residual mean mass stream function. Absolute angular momentum per unit mass is shown by blue contours with contour intervals of 1.0×10^8 $\mathrm{m^2 s^{-1}}$.

References

[1] Greybush, S. J. *et al.* The Ensemble Mars Atmosphere Reanalysis System (EMARS) Version 1.0. *Geoscience Data Journal* **6**, 137–150 (2019).

[2] Kuroda, T., Medvedev, A. S., Yiğit, E. & Hartogh, P. *Geophysical Research Letters* **42**, 9213–9222 (2015).

[3] Sato, K. & Hirano, S. *Atmospheric Chemistry and Physics* **19**, 4517–4539 (2019).

[4] Asumi, A., Sato, K., Kohma, M. & Hayashi, Y.-Y. *Journal of Geophysical Research: Planets* **130**, e2023JE008137 (2025), doi:10.1029/2023JE008137

[5] Asumi, A., Sato, K. & Hayashi, Y.-Y. (2025) doi:10.22541/essoar.174646106.69644979/v1.